Dynamic-MRI quantification of abdominal wall motion and deformation during breathing and muscular contraction

Arthur Jourdan, Stanislas Rapacchi, Maxime Guye, David Bendahan, Catherine Masson, Thierry Bège

Dynamic-MRI quantification of abdominal wall motion and deformation during breathing and muscular contraction

Arthur Jourdan [a], Stanislas Rapacchi [b], Maxime Guye [b,c], David Bendahan [b], Catherine Masson [a] & Thierry Bège [a,d]

a. Aix-Marseille Univ, Univ Gustave Eiffel, IFSTTAR, LBA, F-13016 Marseille, France

b. Aix Marseille Univ, CNRS, CRMBM, Marseille, France

c. APHM, Hopital Universitaire Timone, CEMEREM, Marseille, France

d. Department of General Surgery, Aix Marseille Univ, North Hospital, APHM, Marseille, France

Corresponding author

Arthur Jourdan : 0000-0001-8656-4066
arthur.jourdan@univ-eiffel.fr
Université Gustave Eiffel, Faculté de Médecine—Secteur Nord, Boulevard P. Dramard, 13916, Marseille Cedex 20, France.

Authors

Stanislas Rapacchi : 0000-0002-8925-495X
stanislas.rapacchi@univ-amu.fr

Maxime Guye : 0000-0002-4435-2257
maxime.guye@univ-amu.fr

David Bendahan : 0000-0002-1502-0958
david.bendahan@univ-amu.fr

Catherine Masson : 0000-0003-3578-9067
catherine.masson@univ-eiffel.fr

Thierry Bège : 0000-0002-0775-3035
thierry.bege@ap-hm.fr

Abstract

Background and Objective: Biomechanical assessment of the abdominal wall represents a major prerequisite for a better understanding of physiological and pathological situations such as hernia, post-delivery recovery, muscle dystrophy or sarcopenia. Such an assessment is challenging and requires muscular deformations quantification which have been very scarcely reported *in vivo*. In the present study, we intended to characterize abdominal wall deformations in passive and active conditions using dynamic MRI combined to a semi-automatic segmentation procedure.

Methods: Dynamic deformations resulting from three complementary exercises i.e. forced breathing, coughing and Valsalva maneuver were mapped in a transversal abdominal plane and so for twenty healthy volunteers. Real-time dynamic MRI series were acquired at a rate of 182ms per image, then segmented semi-automatically to follow muscles deformation through each exercise. Circumferential and radial strains of each abdominal muscle were computed from the geometrical characteristics' quantification, namely the medial axis length and the thickness. Muscular radial displacement maps were computed using image registration.

Results: Large variations in circumferential and radial strains were observed for the lateral muscles (LM) but remained low for the rectus abdominis muscles (RA). Contraction phases of each exercise led to LM muscle shortening down to -9.6 ± 5.9 % during Valsalva maneuver with a 16.2 ± 9.6 % thickness increase. Contraction also led to inward radial displacement of the LM up to 9.9 ± 4.1 mm during coughing. During maximal inhalation, a significant 10.0 ± 6.6 % lengthening was quantified for LM while a significant thickness decrease was computed for the whole set of muscles (-14.7 ± 6.6 % for LM and -7.3 ± 6.5 % for RA). The largest displacement was observed for the medial part of RA (17.9 ± 8.0 mm) whereas the posterior part of LM underwent limited motion (2.8 ± 2.3 mm). Displacement rate and correlation between muscle thickness and medial axis length during each exercise provided insights regarding subject-specific muscle function.

Conclusions: Dynamic MRI is a promising tool for the assessment of the abdominal wall motion and deformations. The corresponding metrics which have been continuously recorded during the exercises provided global and regional quantitative information. These metrics offer perspectives for a genuine clinical evaluation tool dedicated to the assessment of abdominal muscles function in both healthy subjects and patients.

Keywords

Abdominal wall, Muscles, Biomechanics, Dynamic magnetic resonance imaging, Deformations, Geometrical characteristics

Abbreviations

RA : rectus abdominis; TA : transversus abdominis; IO : internal obliquus; EO : external obliquus; LM : lateral muscles; WC : waist circumference; BMI : body mass index; r : Pearson correlation coefficient; DSC : Dice similarity coefficient; HD : Hausdorff distance (HD); ICC : intraclass correlation coefficient; SD : standard deviation; EMG : electromyography;

1. Introduction

From a physiological point of view, the abdominal wall is a flexible and resistant interface which delimits the intra-abdominal cavity (Figure 1). This complex multi-layered structure plays a central role in breathing, intra-abdominal pressure (IAP) regulation, protection of the internal abdominal organs and stabilization and rotation of the trunk.

Biomechanical assessment of the abdominal wall represents a major prerequisite for a better understanding of any situation involving abdominal muscle deficiency such as hernia, post-delivery recovery, muscle dystrophy or sarcopenia. A complete evaluation of the abdominal wall requires to assess both the mechanical properties of muscles and aponeurotic tissues, the function of those tissues under different loading conditions and the coupling between the two. Such an evaluation can be challenging and requires various stimulations through multiples exercises, with in-depth observations, including continuous IAP monitoring and deformations quantification, to unveil the structure-function coupling.

Ideally, one would need information related to mechanical properties of the muscular and aponeurotic tissues of the abdominal wall under passive conditions and during muscle activation. It could also be of interest to investigate the IAP in order to determine the mechanical stresses applied to the wall. Finally, it would be essential to assess and quantify the motion of the abdominal wall to determine the levels of tissues deformations.

Over the past few years, multiple studies have been devoted to muscle and aponeurotic tissues characterization and to IAP. Mechanical properties of the linea alba (1–5) together with anterior and posterior sheath of the rectus abdominis (1,6–8) and abdominal muscles (9–11) have been assessed *ex vivo*. Those studies highlighted the anisotropic and hyperelastic behavior of the abdominal wall soft tissues, the importance of the connective tissues in the structural response of the abdominal wall and their higher stiffness in the transverse direction compared to the cranio-caudal. Mechanical properties of abdominal wall muscles have also been investigated *in vivo* during activation (12) revealing that local stiffness of the abdomen was related to muscle activity. Specific muscle activation patterns have been identified (13–15) using electromyography (EMG). A major recruitment of the lateral abdominal muscles (LM) i.e. transversus abdominis (TA), internal obliquus (IO) and external obliquus (EO) compared to rectus abdominis (RA) during coughing, voluntary abdominal contraction (Valsalva maneuver) and forced exhalation has been reported (13–15). Coughing and Valsalva maneuver in supine position have been shown to increase IAP up to 40 mmHg (16) and higher.

However, in-vivo human abdominal wall deformations studies remain scarce. The few existing studies have used ultrasound imaging and surface tracking. Using ultrasound imaging, abdominal muscle thickness has been measured at different contraction levels (17–19) showing that TA and IO were thicker at the end of expiration and that muscle thickness was correlated with muscle activation. Abdomen surface deformation has been assessed using external markers tracking during passive insufflation, Valsalva maneuver, stretching, bending and trunk torsion.

During passive insufflation, the abdominal wall shape changed from a cylinder to a dome and maximal displacement up to 40mm were observed at the center of the abdomen (20). Valsalva maneuver induced raising of the abdominal surface in the region adjacent to linea alba along the posterior-anterior direction and a simultaneous lowering along lateral-medial direction of the abdominal wall sides (21). The largest reported displacement was 12.5 mm in the anterior direction. During stretching, bending and trunk torsion, strains larger than 25% were observed in the upper part of the central vertical line of the abdomen and in lower sides in semi-vertical direction (22). Although these studies provided valuable information regarding deformation of the abdomen under passive and active conditions, they were limited to a surface analysis and did not quantify deformations of the deep tissues which could be involved in abdominal wall deficiency i.e. muscles and aponeurotic sheaths.

Dynamic MRI, also referred as cine MRI, which consists in repeatedly imaging the area of interest, is a powerful and versatile non-invasive modality for the quantification of abdominal wall deformations. Such an imaging modality is of interest given that, unlike ultrasound and surface analysis, it allows dynamic monitoring of both the superficial and deep components of the abdominal wall. So far, the few dynamic MRI studies of abdominal wall have focused on abdominal wall adhesions after surgery (23–25). To the best of our knowledge, abdominal wall deformations have not yet been investigated using dynamic cine MRI.

In the present study, we intended to investigate a complete protocol to characterize abdominal wall deformations in passive and active conditions using dynamic MRI. Dynamic deformations induced by three complementary exercises i.e. forced breathing, coughing and Valsalva maneuver were mapped on a transversal plane of the abdomen. Dynamic muscles changes were individually characterized, namely the medial axis length and thickness and displacements of each abdominal muscles.

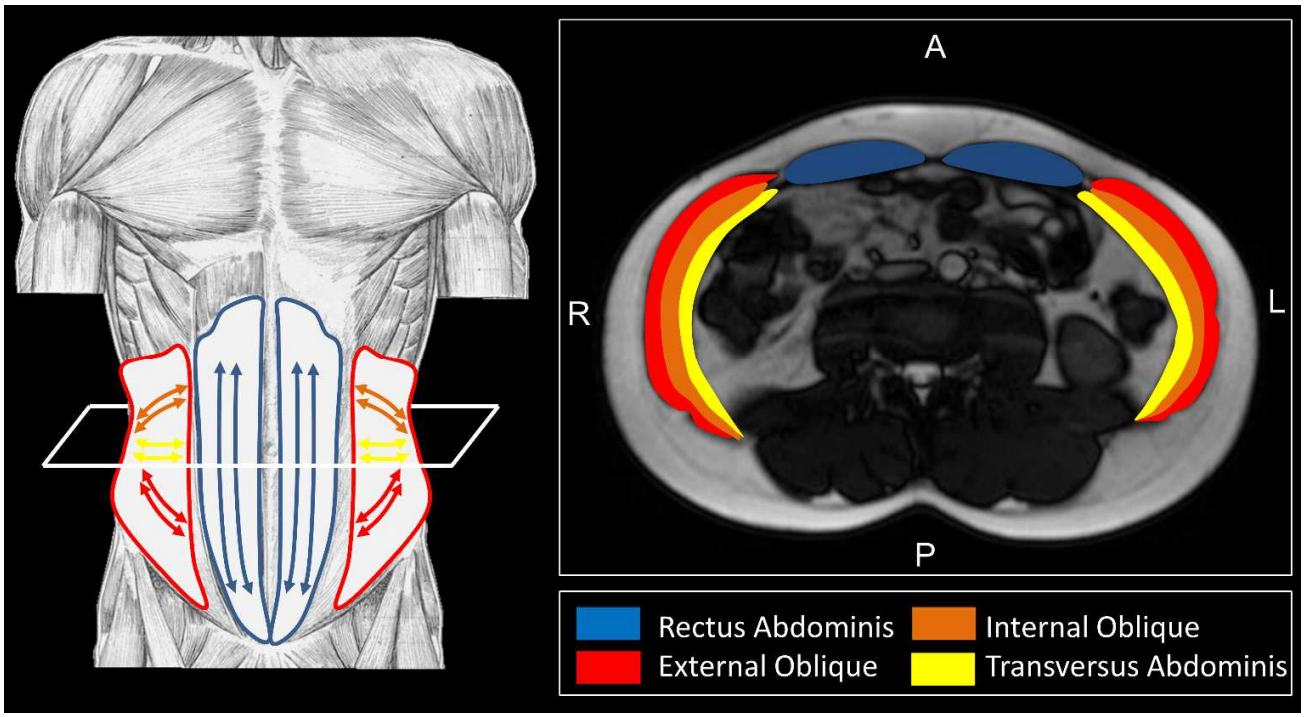

Figure 1 : Abdominal wall muscles and muscle fiber orientation.

2. Subjects and methods

The study was approved by the ethics committee (IDRCB: 2019-A00806-51) and was conducted according to national legislation on interventional research and the declaration of Helsinki.

2.1. Subjects

Twenty healthy subjects (8 women) were included after they provided informed written consent. The exclusion criteria included a history of abdominal or incisional hernia and pathologies involving breathing or digestive functions and any contraindication for MRI. Information related to the subjects' physical activity was gathered. A score related to physical activity was defined as high (at least 6h of physical exercise a week), moderate (2 to 4h a week) or mild (less than 2h a week).

The mean age of the cohort was 30.6 ± 8.7 years, the mean BMI was 22.6 ± 2.4 $kg.m^{-2}$ and the mean waist circumference (WC) was 804 ± 77 mm. 8 volunteers had a high physical activity score, 11 had a moderate score, and 1 had a mild score. Individual characteristics are presented in Table 1.

Table 1 : Subjects characteristics

Subject	Sex	Age (yr)	BMI ($kg.m^{-2}$)	WC (mm)	Physical activity score*
S1	W	23	23.2	786	3
S2	M	24	24.3	849	2
S3	W	26	24.5	850	2
S4	M	27	20.7	697	3
S5	M	25	22.6	750	2
S6	M	25	20.7	723	3
S7	M	27	28.5	978	2
S8	M	26	20.9	732	5
S9	M	41	22.8	856	2
S10	W	28	17.5	678	2
S11	W	29	21.8	807	2
S12	M	27	22.1	792	3
S13	W	22	21.7	788	3
S14	M	37	22.1	825	3
S15	W	30	22.5	755	3
S16	M	28	23.1	823	2
S17	M	47	24.3	921	3

S18	M	41	26.6	896	3
S19	W	24	19.7	720	4
S20	W	54	23.0	845	4

* 1 = High, 2 = Moderate, 3 = Mild

2.2. MRI protocol and exercises

The abdominal region of the participants was imaged in a supine position using a 3T MRI scanner (MAGNETOM Verio, Siemens Healthineers, Erlangen, Germany) with a torso-dedicated 32 channels array coil. Axial images with T1/T2 contrast from a single slice located at the L3-L4 disc level were recorded repeatedly with a temporal resolution of 182 ms using a cine-bSSFP sequence (echo train duration for 1 single-shot image: 182ms, TE/TR: 1.4/3.1 ms, flip angle: 50°, field of view: 360 x 360 mm^2, pixel size: 2.3 x 1.7 mm^2, slice thickness: 8 mm, GRAPPA 4 with 24 reference lines).

Subjects performed 3 stereotyped exercises (guided-breathing, coughing and Valsalva maneuver) within the MRI scanner paced precisely using pre-recorded audio instructions. As a practice session, these exercises were initially performed outside of the MRI room on an examination table and under the supervision of an examiner.

Before each acquisition, the volunteers were instructed to relax their abdominal muscles and breathe calmly. This configuration was considered as the relaxed condition. WC of each subject was measured in relaxed condition.

During the forced breathing session, subjects had to perform three complete breathing cycles including 5s inhalation and 5s exhalation. Subjects were instructed to breathe as steadily as possible while trying to achieve the maximum abdominal amplitude for both inhalation and exhalation phases going from forced inhalation to forced exhalation.

For the coughing session, subjects were asked to cough once after hearing the audio signal. Coughing was repeated 4 times.

For Valsalva maneuver, subjects had to realize a maximal expiratory effort (maximal abdominal muscles contraction) against closed airways after hearing a signal and hold the contraction for 5 seconds. The Valsalva maneuver was repeated twice.

2.3. Image selection

MR images were initially corrected for inhomogeneities using the N4 algorithm as previously described (26). A careful visual inspection was performed in order to make sure that initial images for each exercise type corresponded to a configuration of complete relaxation with no visual activity of the abdominal muscles. If the inspection indicated that an exercise session was not performed according to the indications, the corresponding dataset was discarded.

2.4. Semi-automatic segmentation

We used a semi-automatic segmentation method as previously described (27). Briefly, right and left rectus abdominis (RA) and lateral muscles (LM) as visible in Figure 2 were manually delineated by the same observer in a limited number of slices (five slices for each cycle of the forced breathing sessions i.e. inhalation onset, mid-inhalation, full inhalation, mid-exhalation, and end-inhalation). For the coughing and Valsalva maneuver sessions, three slices were delineated i.e. relaxed conditions, maximum contraction and after relaxation.

The segmented masks were then propagated to the remaining slices using an automatic label propagation algorithm based on image registration, as previously described (28).

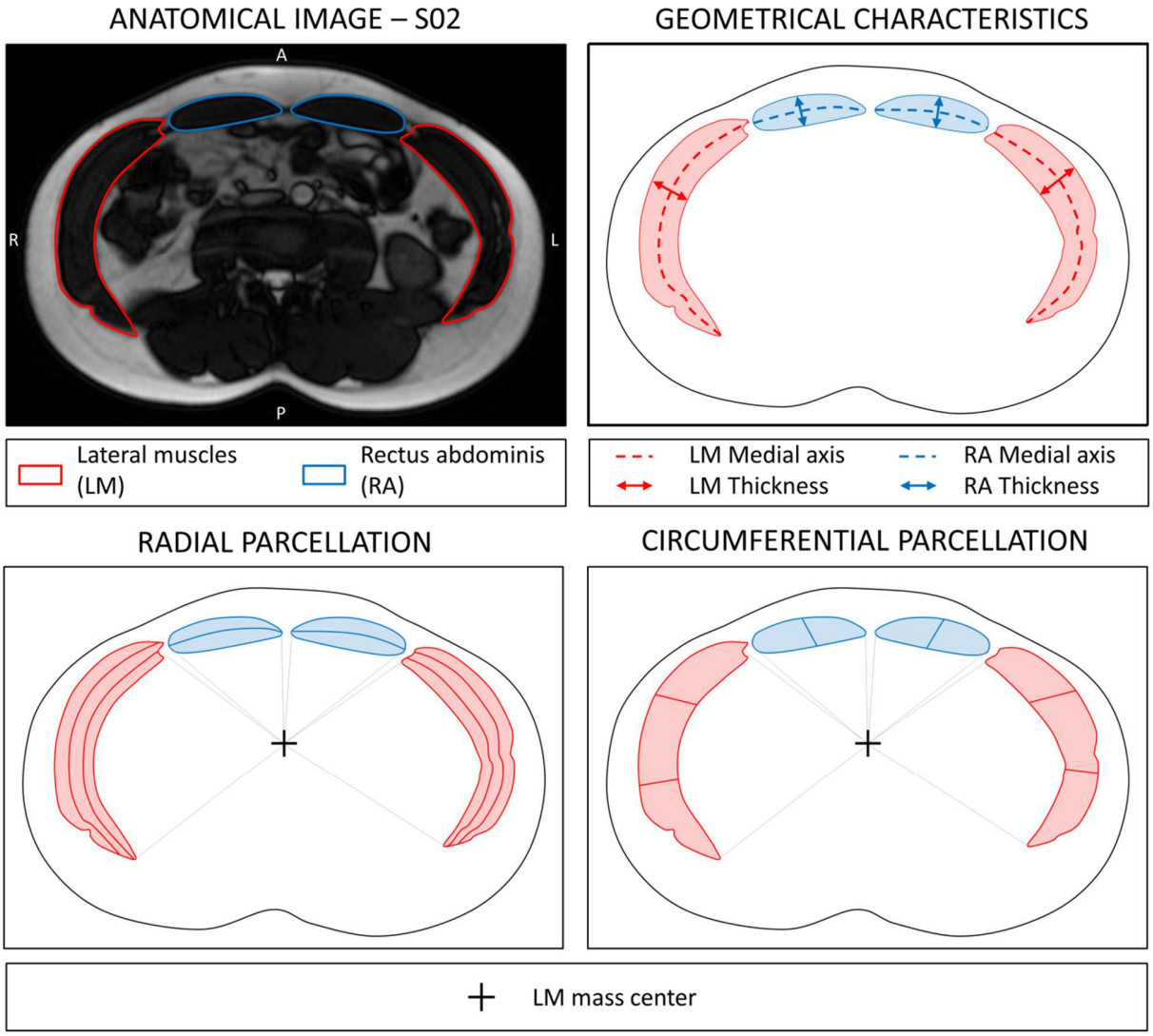

Figure 2: Anatomical cine-MR image of one subject (S02) given as example with lateral muscles (LM) and rectus abdominis (RA) contour delineation; Left and right LM and RA medial axis length and thickness; Radial and circumferential muscle parcellation using a polar coordinate system centered in the lateral muscles mass center.

2.5. Muscles geometrical characteristics and strains

As visible in Figure 2, two geometrical characteristics were assessed for each muscle group. Those characteristics were the medial axis length and the thickness.

In order to calculate the medial axis length for LM and RA, a skeletonization algorithm (29) was used. The longest branch of the "skeleton" was considered as the medial axis of the muscle as illustrated in Figure 2. It is noteworthy that the medial axis length measurement is performed in a direction roughly parallel to the muscle fascicles of LM whereas for RA, this measurement is performed in the direction perpendicular to that of the fascicles which run craniocaudally (*Figure* 1). The medial axis length L_t was measured at each time point and the corresponding circumferential strain ε_c was calculated as follows:

$$\varepsilon_c = \frac{(L_t - L_0)}{L_0}$$

with L_0 refers the medial axis length in relaxed condition.

As can be seen in Figure 2, muscle thickness T_t was calculated as the maximal distance of the medial axis to the muscle contour. The corresponding radial strain ε_r was computed as follows:

$$\varepsilon_r = \frac{(T_t - T_0)}{T_0}$$

with T_0 referring to the muscle thickness in relaxed condition.

For both LM and RA muscles, medial axis length and thickness were compared at different time-points of each exercise session. Non parametric, paired Wilcoxon tests were computed using R Studio (version 1.4.1717). A p-value < 0.05 was chosen as indicative of a statistical significance. Correlation between medial axis length and thickness during exercise sessions was assessed using Pearson's linear correlation coefficient (r) for each subject.

2.6. Muscles radial displacement

The abdominal wall muscles displacements over time were computed on the basis of a registration procedure (27). The registrations between the segmented mask corresponding to the relaxed conditions and each segmented mask of the exercise session was computed using a TimeVaryingVelocityField transformation model implemented in the Ants Library (30). These registrations were used to compute the displacement of each pixel of a given muscle with respect to its position in relaxed conditions.

As indicated in Figure 2 (bottom), the radial component of the displacement was computed using a polar coordinates system for which the center corresponded to the mass center of the lateral muscles (RLM, LLM).

To assess the subjects' compliance regarding radial displacements throughout the various exercises and more specifically the corresponding repeatability, we compared, within each

exercise session, displacements quantified for maximal exhalation, maximal inhalation, cough and Valsalva. This repeated comparative analysis was performed for both LM and RA using a Wilcoxon paired test with appropriate Bonferroni corrections.

2.7. Segmentation and metrics evaluation

To assess the quality of the segmentation propagation process, 2 images per volunteer and per exercise (total of 120 images) were randomly selected and manually segmented. Those manual segmentations were compared to the corresponding propagated segmentation based on the computation of Dice similarity coefficient (DSC) and the Hausdorff distance (HD) defined as the maximum surface distance between the objects.

On the same slices, medial axis length and thickness values were computed for both manual and propagated segmentations and compared using the intraclass correlation coefficient (ICC).

2.8. Individual muscles parcellation

A dedicated automatic parcellation of the segmented masks was performed, as previously reported (27). A polar coordinates system for which the center referred to the mass center of the lateral muscles (RLM, LLM) was used in order to determine the position of each voxel of the segmented masks. On that basis, LM were automatically split radially into three depth layers (superficial, intermediate, and deep) and circumferentially into three angular levels (posterior, central and anterior), as illustrated in Figure 2. The RA ROIs were split into two depths (superficial and deep) and two angular (medial and lateral) levels.

3. Results

3.1. Image selection and manual segmentation

MR images and muscle segmentation of the three exercises are visible in Figure 3, for one subject given as an example.

7% of the initially acquired images were discarded after visual inspection because the exercises had not been correctly performed by the subjects.

The averaged forced breathing cycle was 9.2 ± 0.8 s with a 4.4 ± 0.7 s inhalation and 4.8 ± 0.8 s exhalation phases. The averaged coughing cycle was 1.7 ± 0.7 s with contraction and relaxation phases lasting 0.5 ± 0.2 s and 1.2 ± 0.6 s respectively. The averaged Valsalva cycle was 7.2 ± 0.9 s with a 1.1 ± 0.6 s contraction, a 4.6 ± 0.7 s contraction plateau and a 1.4 ± 0.7 s relaxation.

3.2. Segmentation and metrics evaluation

Manual delineation of LM and RA was performed for 8% of the total slices. Segmentation propagation resulted in an average DSC score of 0.93 ± 0.04 and HD of 3.8 ± 2.2 mm considering the whole set of muscles.

Comparison of medial axis length and thickness measurement on both manual and propagated segmentations resulted in a very high ICC (0.99 for medial axis length and 0.98 for thickness) indicating that the repeated measurements could be considered equivalent.

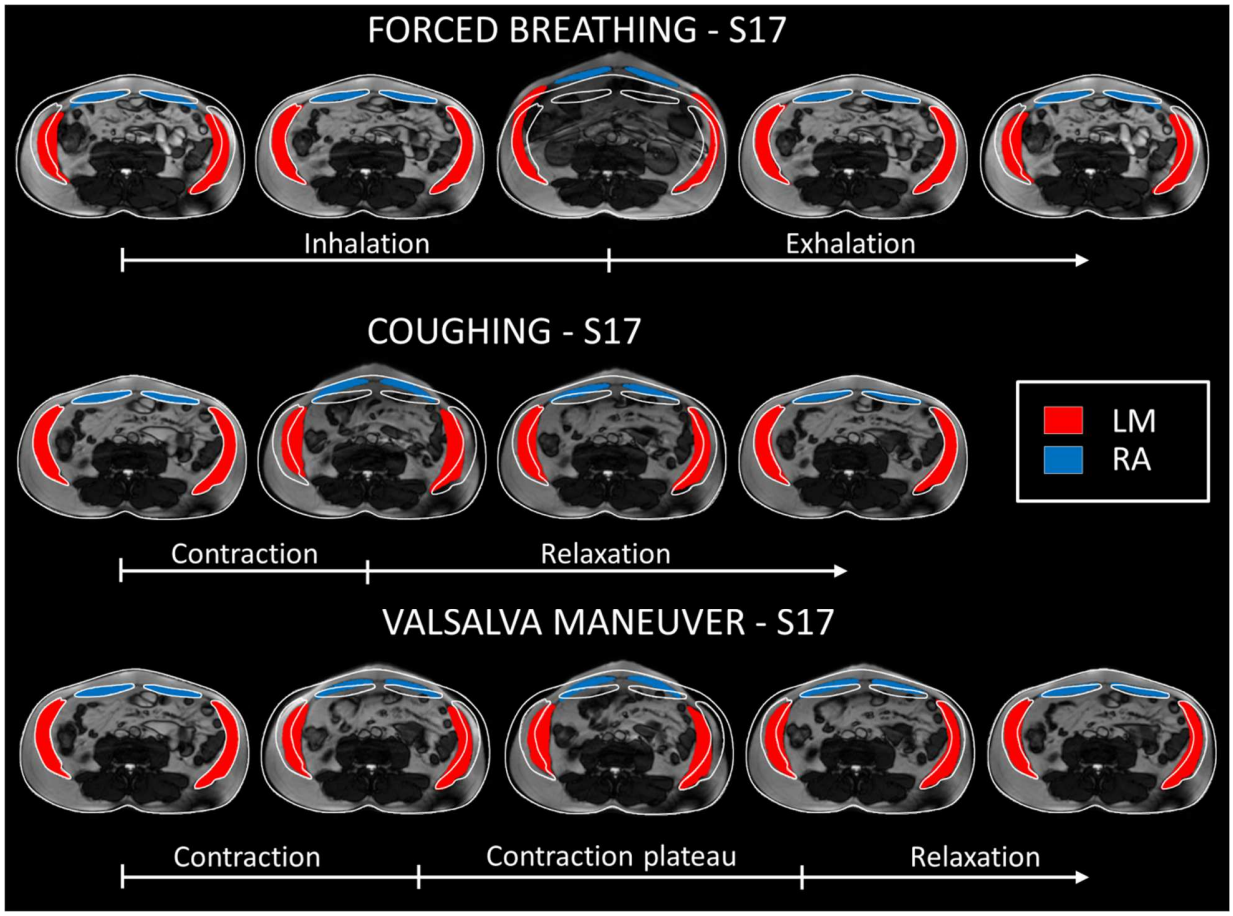

Figure 3 : MR images and segmentation masks for forced breathing, coughing and Valsalva for one subject (S17) given as example; On the MR images, the white lines represent the abdominal circumference and abdominal muscle delineation in relaxed condition.

3.3. Geometrical characteristics and strains

Muscles circumferential and radial strains evolutions with respect to time are illustrated in Figure 4 for the whole cohort. Individual curves were normalized to the average duration of exercise phases measured for the cohort. The average curve is presented with corridors representing ± one standard deviation. Average muscle medial axis length and muscle thickness values in relaxed conditions, end-inhalation, end-exhalation and at maximal contraction during coughing and Valsalva maneuver are gathered in Table 2. The data presented are averaged between the left and right LM and left and right RA.

During forced inhalation, LM medial axis length significantly increased from -8.4 ± 6.2 % at inhalation onset to 10.0 ± 6.6 % at the end of inhalation (Figure 4). There was a slight increase of

RA medial axis length from -0.8 ± 5.3 % up to 1.1 ± 5.6 % but no statistically difference was observed. At the same time, muscles thicknesses decreased significantly: LM thickness decreased from 9.7 ± 11.5 % to -14.7 ± 6.6 % and RA thickness decreased from -0.5 ± 7.6 % to -7.3 ± 6.5 %. During the forced exhalation phase, both medial axis length and thickness gradually returned to their initial value and so for both muscles.

During the contraction phase of the coughing session, one could observe a significant shortening of LM (-7.0 ± 4.9 %) whereas the RA medial axis length remained longer as compared to the relaxed conditions. At the same time, LM thickness significantly increased up to 10.1 ± 9.4 %. There was no significant change for the RA thickness. As illustrated in Figure 4, the relaxation phase was characterized by a normalization of both medial axis length and thickness for the LM muscle.

During Valsalva, LM medial axis length was shortened by -9.6 ± 5.9 % whereas a 16.2 ± 9.6 %. LM thickness increase was quantified. These variations were globally constant during the contraction session and were reversed during the relaxation part. RA medial axis length was significantly higher during contraction (+3.0%) with respect to relaxed conditions but no change of the RA thickness was observed.

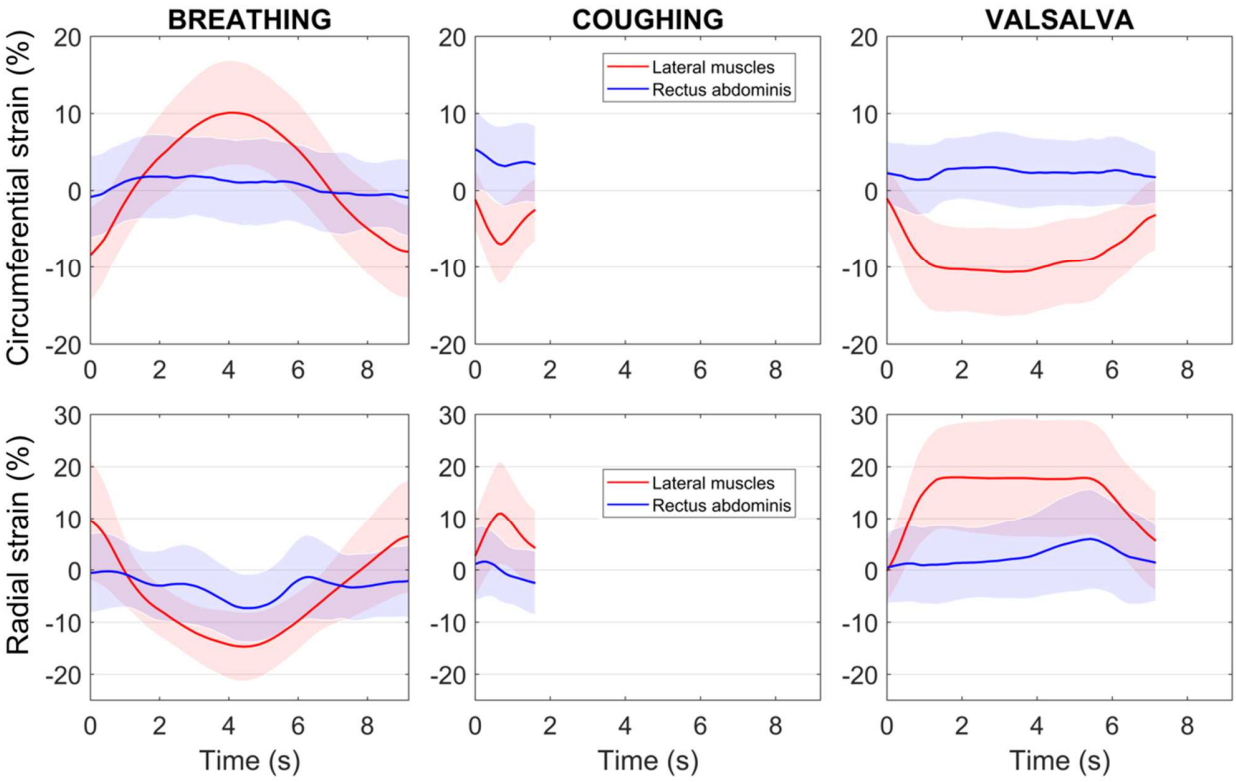

Figure 4: Average time-dependent evolution of muscle circumferential and radial strains with respect to relaxed conditions while forced breathing, coughing and Valsalva for the whole cohort; the shaded areas represent one standard deviation.

	Relaxed	End-exhalation		End-inhalation		Coughing		Valsalva	
			p^*		p^*		p^*		p^*
Medial axis length (mm)									
LM	148.7	140.6	*<0.001*	166.8	*<0.001*	141.4	*<0.001*	131.2	*<0.001*
RA	61.6	61.3	*0.388*	62.3	*0.235*	63.3	*<0.001*	63.7	*0.022*
Thickness (mm)									
LM	26.4	28.7	*<0.001*	22.4	*<0.001*	28.4	*<0.001*	30.2	*<0.001*
RA	14.5	14.5	*0.767*	13.5	*<0.001*	14.6	*0.583*	14.7	*0.068*

** with respect to relaxed conditions*

Table 2 : Medial axis length and thickness of lateral muscles and rectus abdominis in relaxed conditions, at end-inhalation, end-exhalation and at maximal contraction during coughing and Valsalva.

Correlations between medial axis length and thickness during forced breathing, coughing and Valsalva are illustrated in Figure 5 for a typical subject and so for both muscles. The elevated r values illustrated strong inverse correlations for LM muscles during forced breathing (r = -0.86 ± 0.17) and moderate correlations during coughing (r = -0.64 ± 0.26) and Valsalva (r = - 0.67 ± 0.36). The corresponding correlations were low for RA muscles with r = - 0.05 ± 0.28 for forced breathing, r = 0.26 ± 0.38 for coughing and r = 0.01 ± 0.39 for Valsalva. Averaged slope and y-intercept for the whole cohort are reported in Table 3.

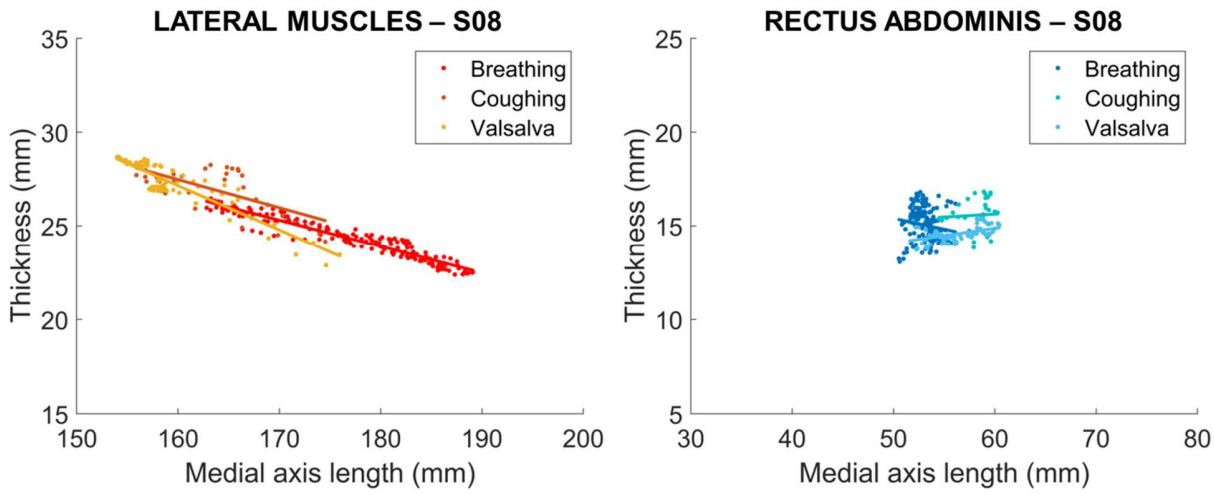

Figure 5 : Medial axis length and thickness correlation for lateral muscles and rectus abdominis of one subject (S08) given as example; linear regression curves are presented for each exercise.

Table 3 : Pearson correlation coefficient, slope and y-intercept of muscle medial axis-length vs thickness linear regression for the whole cohort.

	Lateral muscles			Rectus abdominis		
Exercise	***r***	**Slope***	**y-intercept***	***r***	**Slope***	**y-intercept***
Breathing	*- 0.86±0.17*	-0.20±0.10	54.54±16.88	*-0.05±0.28*	-0.02±0.10	14.75±6.18
Coughing	*-0.64±0.26*	-0.18±0.10	53.15±17.13	*0.26±0.38*	0.09±0.17	8.39±10.77
Valsalva	*- 0.67±0.36*	-0.24±0.18	61.28±27.56	*0.01±0.39*	- 0.01 ± 0.22	15.27±13.87

** In the linear regression equation $y = a * x + b$, a is the slope and b the y-intercept*

3.4. Muscles radial displacement

Radial displacement maps at maximal inhalation, in maximal contraction, coughing and Valsalva are illustrated in Figure 6 for four subjects given as examples. Individual curves were normalized to the average duration of exercise phases measured for the cohort. The average radial displacement of muscles parcels over time for the whole cohort is displayed in Figure 7.

Inhalation led to a significant increase of radial displacement of each parcel up to 17.9 ± 8.0 mm observed in the medial RA parcel and a minimum of 2.8 ± 2.3 mm in the posterior LM parcel. The radial parcellation showed that the deepest area of LM was submitted to larger displacements as compared to the superficial one. Inhalation onset configuration (i.e. end-exhalation) was significantly different than relaxed conditions as all parcels presented negative radial displacement from – 5.0 ± 4.9 mm for the medial RA parcel to – 3.1 ± 3.5 mm for the posterior LM parcel. Radial displacements during exhalation and inhalation phases were relatively symmetrical for all parcels.

Both contraction phases of coughing and Valsalva led to negative radial displacement of the LM parcels. Those displacements were maximal in the central LM parcel (-10.5 ± 4.1 mm in coughing and -9.8 ± 3.9 mm in Valsalva). The deep LM parcel was subjected to a higher displacement (-9.9 ± 4.1 mm in coughing and -9.7 ± 4.2 mm in Valsalva) than the one quantified in the superficial one (-7.3 ± 3.2 mm for Valsalva and -7.9 ± 3.4 mm for coughing). However, these displacements were achieved on average twice as fast when coughing (0.5s and 1.1s for coughing and Valsalva respectively). Average displacement rate during contraction was -18.9 ± 6.5 $mm.s^{-1}$ for LM during coughing and -9.1 ± 4.7 $mm.s^{-1}$ during Valsalva. During Valsalva there was a progressive positive radial displacement of the RA parcels that reached its maximum approximatively at the half of the contraction plateau up to 4.8 ± 4.6 mm in the medial RA parcel. During coughing, RA

underwent very limited motion. During Valsalva, the maximal contraction was maintained on average 4.6s before relaxation. When coughing, relaxation started right after maximal contraction was reached. During relaxation, muscles returned to the initial relaxed conditions.

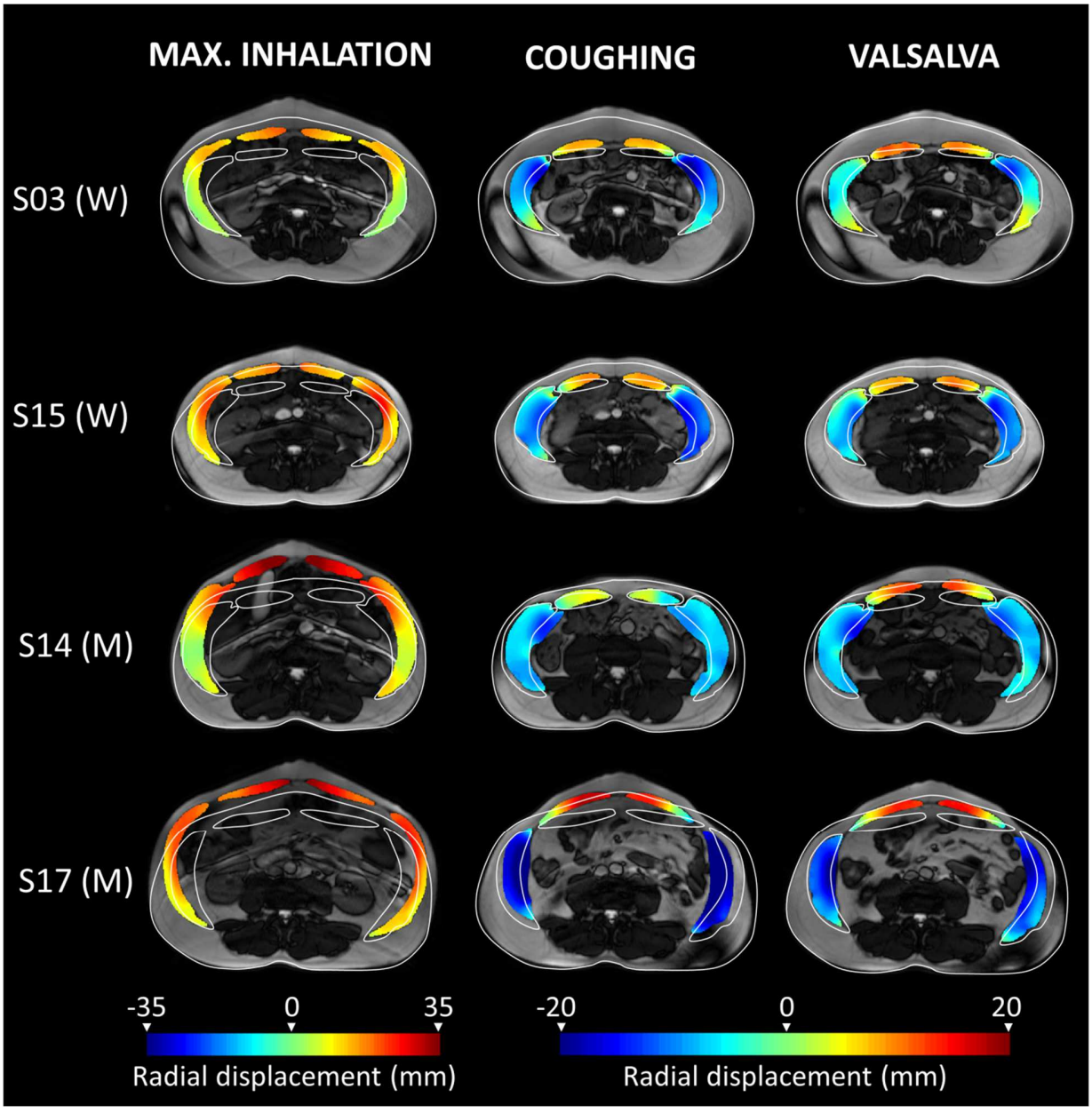

Figure 6 : MR images and muscles radial displacement maps of 4 subjects given as example (2 women : S03, S15 and 2 men : S14, S17) in maximal inhalation, coughing and Valsalva; the white lines represent the abdominal circumference and abdominal muscle delineation in relaxed condition.

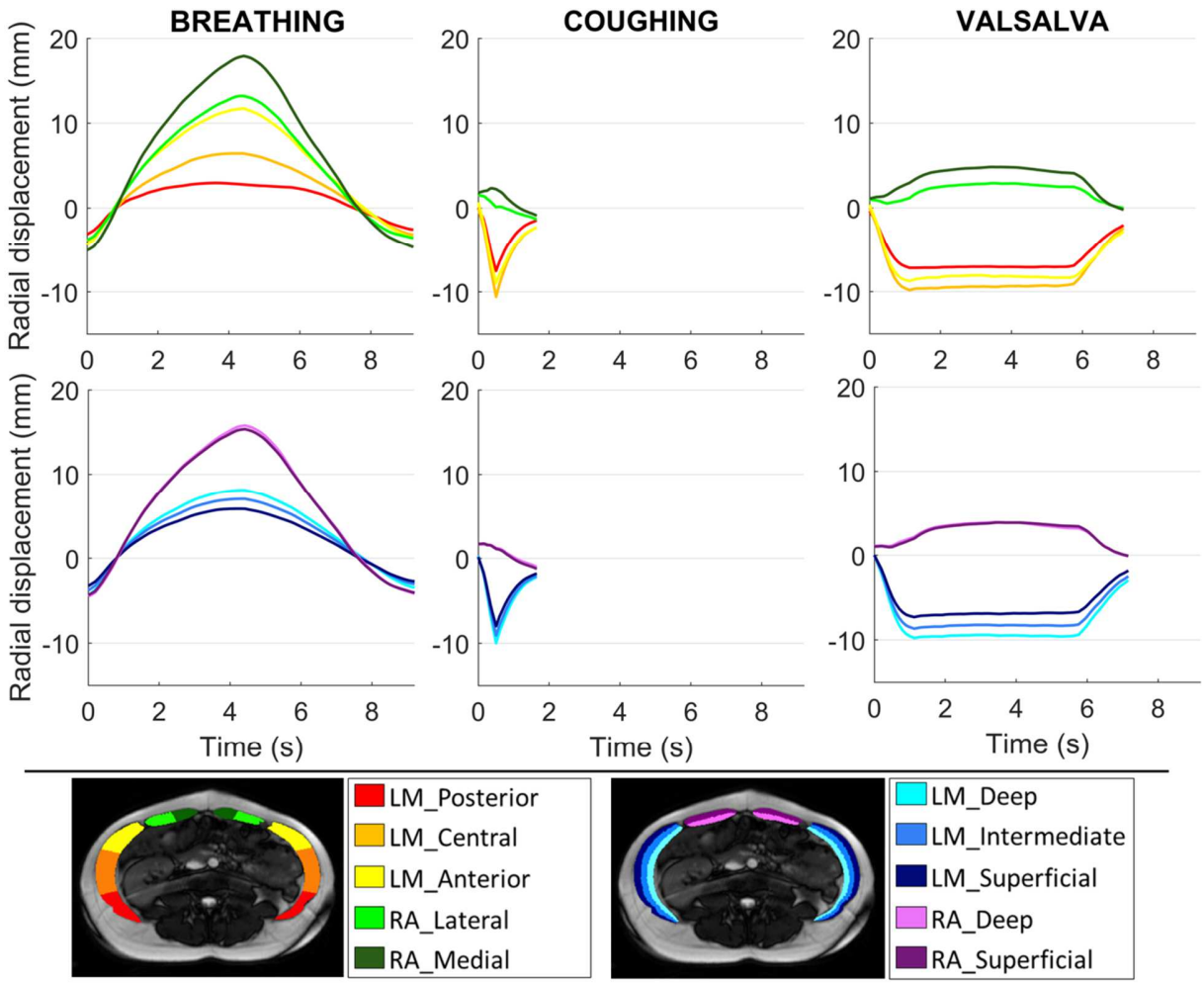

Figure 7: Average time-dependent evolution of muscle radial displacement within parcels while forced breathing, coughing and Valsalva for the whole cohort; the parcels nomenclature is detailed at the bottom of the figure.

The statistical analysis for the evaluation of the exercises repeatability regarding radial displacement of LM and RA disclosed no difference for maximal exhalation, maximal inhalation and cough. Only the RA radial displacement quantified during the repeated Valsalva maneuvers was different ($p<0.001$). For each volunteer, the standard deviation (SD) of the displacement values measured at each repetition was also measured and averaged for the whole group. For the LM displacements, the averaged SD was 0.8 mm in maximal exhalation, 0.8 mm in maximal inhalation, 0.7 mm for coughing and 1.1 mm for Valsalva. For the RA displacements, the averaged SD was 1.2 mm in maximal exhalation, 1.7 mm in maximal inhalation, 1.5 mm for coughing and 1.6 mm for Valsalva.

Discussion

In this study, dynamic MRI was combined to an original image processing framework to map abdominal wall deformations dynamics under three complementary exercises : forced breathing, coughing and Valsalva maneuver. A dedicated quantification of muscle geometry and motion metrics, namely medial axis length, thickness and radial displacement, was presented and permitted to synthetize the structural and functional status of individual abdominal wall muscles. This is, to our knowledge, the first study to provide quantitative temporal data in humans in vivo and so for all the muscles of the anterolateral wall.

Dynamic assessment of the geometrical characteristics of the muscles unlocked key information for the understanding of the function and role of the different muscles of the abdominal wall, with highly reliable measurements (ICC > 0.98). Abdominal wall muscles thickness has been shown to correlate with muscular activation(17–19). In this work, for all exercises, important changes in medial axis length and thickness were observed for the LM but remained low for RA (table 2). This observation suggested the limited solicitation of RA compared to a higher activation of LM, in line with observations from P. Neumann et al. (14) reporting a much larger recruitment of LM (85% of normalized EMG) compared to RA (14%) during the same exercises. However, the transverse plane which has been imaged in this work was roughly parallel to the LM muscle fascicles whereas it was perpendicular to the RA fascicles which run cranio-caudally (31). This could explain why higher medial axis length variations (i.e. circumferential strain) occurred during contraction in LM in comparison to RA, as LM fascicle shortening implied a reduction of the muscle length in the imaging plane.

Taking a closer look at the evolution of circumferential and radial strains during the exercises, several parallels with the literature could be made. Forced breathing is an exercise in which passive and active phases of the abdominal muscles alternate. A previous study using EMG has shown that during inhalation, the abdominal muscles remained passive and demonstrated negligible activity during exhalation, until the lung volume had almost returned to its resting level (32). At this time, LM activity occurred and became increasingly pronounced until maximal exhalation was reached. From Figure 4 the same distinction between active and passive phases of abdominal muscles could be made. It was visible that during inhalation, abdominal muscles lengthened and thinned, demonstrating no muscular activation. However during exhalation, the onset of LM muscular contraction during exhalation was clearly identifiable on the graph at 7.5s (i.e. middle of the exhalation cycle as guided by audio instructions). It corresponded to the simultaneous increase of LM thickness above the relaxed thickness (i.e. radial strain > 0%) and a decrease of the medial axis length below the relaxed length (i.e. circumferential strain < 0%). Another study using ultrasound imaging quantified a 6% thickening of the LM during a normal exhalation (17). In this study, we also observed a significant thickening of the LM but it was more important (> 20%) because maximal exhalation was performed. Coughing and Valsalva are also

muscle contraction exercises. In this study they also led to a significant shortening and thickening of the LM that we were able to quantify.

Circumferential and radial strains were measurable in the present study and could open up new investigational fields. Using cardiac MRI, measurement of radial and circumferential strain have allowed the identification of myocardium regional alterations (33). In the same way, dynamic measurements reported in the present study could allow the localization of regional deficiencies of the abdominal wall.

Linear regression between medial axis length and thickness showed good correlations for LM (Figure 5 and Table 3). For the three exercises, LM correlation coefficients were -0.64, -0.67 and -0.86 for coughing, Valsalva and forced breathing respectively. Slopes were similar for the whole set of exercises (-0.20 ± 0.10 for breathing, -0.18 ± 0.10 for coughing and -0.24 ± 0.18 for Valsalva). These results indicated that the relation between LM thickness and medial axis length is strong and constant, independently of muscles being passive, relaxing or contracting, whether with high or low velocity. Measuring these slopes are potential biomarkers in further studies for individual performance index of LM muscle function. Considering that muscle geometrical characteristics are strongly correlated with maximum muscle strength and power (34), this performance index could be used for the detection of abdominal muscles pathological changes. Correlations for RA were poor for all three exercises (between -0.05 and 0.26). The small RA thickness and limited medial axis length strains in the axial plane potentially reduce the sensitivity of the methods to probe RA compared to LM. The complementary observation of the RA in the sagittal plane could be of interest.

Similarly to geometrical characteristics, radial displacements were also very informative about abdominal muscles dynamics. During forced breathing, passive deformation resulted in significant positive radial displacements. Those displacements were maximal in the medial RA parcel (17.9 ± 8.0 mm) and minimum in the posterior LM parcels (2.8 ± 2.3 mm). The study by Song et al. (20) found a similar displacements distribution during a 5 mmHg passive insufflation of the abdominal wall in laparoscopic surgery. A maximal 40 mm displacement in the anterior direction at the center of the abdomen was reported while markers at the edge of the abdominal wall underwent very limited motion (< 5 mm) likely resulting from their proximity to the insertions of the abdominal muscles on the ribs.

The computation of the radial displacement during contraction resulted in negative radial displacements of the LM relative to their relaxed position and a positive displacement of the RA toward the front (Figure 6 and Figure 7). The Valsalva maneuver induced a – 9.8 ± 3.9 mm displacement of the central LM parcel. Using surface analysis, Todros et al. (21) observed in low or normal BMI subjects a similar raising of the abdomen surface in the central zone in the posterior-anterior direction and a simultaneous lowering along lateral-medial direction of the abdominal wall sides with a maximum of - 12.5 mm. While skin surface analysis correctly

predicted the deep abdominal muscles displacement during contraction in Todros study, a thicker adipose layer might hamper this evaluation. MRI analysis does not present this limitation.

Radial parcellation of the LM in Figure 7, provided new insights regarding the muscle regions most involved in the contraction phase. Indeed, at maximal contraction, the average radial displacement in the LM deep parcel (-9.7 ± 4.2 mm for Valsalva and -9.9 ± 4.1 mm for coughing) was superior to the radial displacement of LM superficial parcel (-7.3 ± 3.2 mm for Valsalva and -7.9 ± 3.4 mm for coughing). This could reflect a larger activation of the deep LM muscle (i.e. TA) as compared to the superficial one (i.e. EO). These findings are supported by those from P. Neumann (14) using EMG. They reported a larger recruitment of TA (66% and 179% of normalized EMG for Valsalva and coughing respectively) compared to EO (6% and 56% of normalized EMG for coughing and Valsalva respectively).

As mentioned previously, the radial displacement values at maximal contraction were roughly similar in Valsalva and coughing. However, coughing resulted in a twice as fast displacement rate of LM than Valsalva (-18.9 ± 6.5 $mm.s^{-1}$ and -9.1 ± 4.7 $mm.s^{-1}$ respectively). Previous studies indicated that both exercises generated high IAP (16,35). Yet coughing has been reported to generate significantly higher IAP values (81.4 ± 25.6 mmHg) as compared to Valsalva (39.7 ± 11.0 mmHg) (16). As a result, contraction velocities could be correlated to IAP. High contraction velocities could be deleterious, especially after surgery, because they generate important mechanical loads on the aponeurosis and the muscles (36). In addition, displacement rate could be a useful metrics for the assessment of muscle function, as previous studies have shown that the maximal shortening velocity was lower in injured muscles (37). These observations warrant further evaluation in the clinics.

Segmentation was a key step in the post-processing method as geometrical characteristics and displacement were computed from the segmentation masks. An efficient LM and RA semi-automatic 2D+t segmentation method on dynamic MRI was reported. The quality of the automatic segmentation propagation was evaluated from a comparative analysis with manual segmentations performed by an expert and using similarity metrics, namely DSC and HD. The resulting DSC and HD scores were 0.93 ± 0.04 and 3.8 ± 2.2 mm respectively while 90% of the manual segmentation effort was spared. In previous studies, deep-learning based automatic segmentation of abdominal muscles on 3D CT scans (38) has shown comparative results (DSC = 0.96 ± 0.02). However to our knowledge, no other automatic or semi-automatic segmentation of abdominal muscles on MRI or dynamic-MRI data has been reported. Abdominal muscles 2D+t segmentation remains very challenging, because large and rapid deformations and changes in muscle shape occurred. In addition, muscles and visceral organs sometimes shared similar texture and intensity, which made segmentation potentially challenging whenever visceral organs approached muscles during exercises. In all cases, the semi-automatic segmentation method proved its efficiency and robustness on all three exercises. Nevertheless, a complete automated segmentation process, leveraging deep learning methods to initiate muscles segmentation could be of interest.

The complementary exercises studied in this work proved to be very reproducible, supporting the potential for clinical investigations. The average standard deviation (SD) of the displacement values measured at each repetition was below 1.1 mm for LM and 1.7 mm for RA for all exercises. The practice session outside of MRI and the pre-recorded audio instructions probably strengthened this reproducibility and should be considered for the future evaluation of subjects.

Several limitations must be acknowledged in the present study. 2D dynamic MRI is limited to the analysis of displacements of organs of interest in a section plane and not in the perpendicular direction. It can be reasonably assumed that abdominal muscles displacements in the cranio-caudal direction are negligible because the muscular insertions on the bone rigid frame are likely to constrain the movements in that direction. In a previous work (27), a ratio of 1/20 between the displacements in the axial plane (i.e. imaged plane) and those in the sagittal plane was found during forced inhalation. The choice of a single axial slice was linked to the high spatial and temporal resolution obtained for dynamic MRI. Such a resolution (~2mm in-plane and 182 ms per image) was necessary to properly assess the exercise dynamics. The axial plane was the only plane allowing the visualisation of the whole set of abdominal muscles at once. For pathological applications, slice location or orientation could be changed, and multi-slice (3D+t) MRI could be considered for selected exercises.

Given the MRI acquisition parameters, the image resolution did not allow to distinguish and delineate the three lateral muscles layers (EO, IO and TA). Thus, only the whole LM was segmented, and geometrical characteristics of each individual muscle could not be measured. As an alternative solution of interest, the radial parcellation of the LM into three layers approached the estimation of individual muscle recruitment.

It could be argued that the physical activity score of our relatively athletic cohort (only one volunteer with mild physical activity score) does not coincide with those of patients with abdominal muscle deficiency. However, the method should also be operational in subjects with various histological changes such as muscle atrophy and fat infiltration since the initial segmentation step is manual. In addition, subjects with a lower physical activity or higher BMI are expected to present thicker subcutaneous and/or visceral fat, which should improve the contrast at the vicinity of the abdominal muscles and therefore facilitate their segmentation.

Conclusion

According to the results of the present study, dynamic MRI can be considered a promising tool for the dynamic assessment of the abdominal wall geometrical characteristics and displacement. The corresponding metrics which have been continuously recorded during forced breathing, coughing and Valsalva maneuver provided global and regional quantitative information. Based

on an in-depth analysis of these metrics, we were able to provide extensive measurements, conventionally obtained separately using intramuscular EMG, ultrasound imaging and/or surface tracking. These metrics offer perspectives for an additional clinical evaluation tool for evaluating abdominal muscles function in both healthy subjects and patients with hernia, post-delivery recovery, muscle dystrophy or sarcopenia.

Acknowledgements

We would like to thank Claire Costes, Lauriane Pini and Patrick Viout (CRMBM/CEMEREM UMR CNRS 7339) for their help in integrating the volunteers and carrying out the MRI acquisitions, Thomas Troalen (Siemens Healthineers) for his assistance in the optimization of the MRI sequences, Pierre Daude and Arnaud Le Troter (CRMBM/CEMEREM UMR CNRS 7339) for their insightful comments on data processing.

Conflict of interest statement

The authors have no conflicts of interest and nothing to disclose.

References

1. Astruc L, De Meulaere M, Witz J-F, Nováček V, Turquier F, Hoc T, et al. Characterization of the anisotropic mechanical behavior of human abdominal wall connective tissues. Journal of the Mechanical Behavior of Biomedical Materials. 2018 Jun 1;82:45–50.

2. Cooney GM, Lake SP, Thompson DM, Castile RM, Winter DC, Simms CK. Uniaxial and biaxial tensile stress–stretch response of human linea alba. Journal of the Mechanical Behavior of Biomedical Materials. 2016 Oct 1;63:134–40.

3. Förstemann T, Trzewik J, Holste J, Batke B, Konerding MA, Wolloscheck T, et al. Forces and deformations of the abdominal wall—A mechanical and geometrical approach to the linea alba. Journal of Biomechanics. 2011 Feb 24;44(4):600–6.

4. Gräβel D, Prescher A, Fitzek S, Keyserlingk DG v., Axer H. Anisotropy of human linea alba: A biomechanical study. Journal of Surgical Research. 2005 Mar 1;124(1):118–25.

5. Levillain A, Orhant M, Turquier F, Hoc T. Contribution of collagen and elastin fibers to the mechanical behavior of an abdominal connective tissue. Journal of the Mechanical Behavior of Biomedical Materials. 2016 Aug 1;61:308–17.

6. Martins P, Peña E, Jorge RMN, Santos A, Santos L, Mascarenhas T, et al. Mechanical characterization and constitutive modelling of the damage process in rectus sheath. Journal of the Mechanical Behavior of Biomedical Materials. 2012 Apr 1;8:111–22.

7. Ben Abdelounis H, Nicolle S, Otténio M, Beillas P, Mitton D. Effect of two loading rates on the elasticity of the human anterior rectus sheath. Journal of the Mechanical Behavior of Biomedical Materials. 2013 Apr 1;20:1–5.

8. Tran D, Mitton D, Voirin D, Turquier F, Beillas P. Contribution of the skin, rectus abdominis and their sheaths to the structural response of the abdominal wall ex vivo. Journal of Biomechanics. 2014 Sep 22;47(12):3056–63.

9. Pachera P, Pavan PG, Todros S, Cavinato C, Fontanella CG, Natali AN. A numerical investigation of the healthy abdominal wall structures. Journal of Biomechanics. 2016 Jun 14;49(9):1818–23.

10. Hernández B, Peña E, Pascual G, Rodríguez M, Calvo B, Doblaré M, et al. Mechanical and histological characterization of the abdominal muscle. A previous step to modelling hernia surgery. Journal of the Mechanical Behavior of Biomedical Materials. 2011 Apr 1;4(3):392–404.

11. Grasa J, Sierra M, Lauzeral N, Muñoz MJ, Miana-Mena FJ, Calvo B. Active behavior of abdominal wall muscles: Experimental results and numerical model formulation. Journal of the Mechanical Behavior of Biomedical Materials. 2016 Aug 1;61:444–54.

12. Tran D, Podwojewski F, Beillas P, Ottenio M, Voirin D, Turquier F, et al. Abdominal wall muscle elasticity and abdomen local stiffness on healthy volunteers during various physiological activities. Journal of the Mechanical Behavior of Biomedical Materials. 2016 Jul 1;60:451–9.

13. Brown SHM, McGill SM. A comparison of ultrasound and electromyography measures of force and activation to examine the mechanics of abdominal wall contraction. Clinical Biomechanics. 2010 Feb 1;25(2):115–23.

14. Neumann P, Gill V. Pelvic Floor and Abdominal Muscle Interaction: EMG Activity and Intra-abdominal Pressure. Int Urogynecol J. 2002 Apr 1;13(2):125–32.

15. Urquhart DM, Hodges PW, Allen TJ, Story IH. Abdominal muscle recruitment during a range of voluntary exercises. Manual Therapy. 2005 May 1;10(2):144–53.

16. Cobb WS, Burns JM, Kercher KW, Matthews BD, James Norton H, Todd Heniford B. Normal Intraabdominal Pressure in Healthy Adults. Journal of Surgical Research. 2005 Dec 1;129(2):231–5.

17. Ainscough-Potts A-M, Morrissey MC, Critchley D. The response of the transverse abdominis and internal oblique muscles to different postures. Manual Therapy. 2006 Feb 1;11(1):54–60.

18. John EK, Beith ID. Can activity within the external abdominal oblique be measured using real-time ultrasound imaging? Clinical Biomechanics. 2007 Nov 1;22(9):972–9.

19. Mew R. Comparison of changes in abdominal muscle thickness between standing and crook lying during active abdominal hollowing using ultrasound imaging. Manual Therapy. 2009 Dec 1;14(6):690–5.

20. Song C, Alijani A, Frank T, Hanna GB, Cuschieri A. Mechanical properties of the human abdominal wall measured in vivo during insufflation for laparoscopic surgery. Surg Endosc. 2006 Jun 1;20(6):987–90.

21. Todros S, de Cesare N, Pianigiani S, Concheri G, Savio G, Natali AN, et al. 3D surface imaging of abdominal wall muscular contraction. Computer Methods and Programs in Biomedicine. 2019 Jul 1;175:103–9.

22. Szymczak C, Lubowiecka I, Tomaszewska A, Śmietański M. Investigation of abdomen surface deformation due to life excitation: Implications for implant selection and orientation in laparoscopic ventral hernia repair. Clinical Biomechanics. 2012 Feb 1;27(2):105–10.

23. Lang RA, Buhmann S, Hopman A, Steitz H-O, Lienemann A, Reiser MF, et al. Cine-MRI detection of intraabdominal adhesions: correlation with intraoperative findings in 89 consecutive cases. Surg Endosc. 2008 Nov 1;22(11):2455–61.

24. Fenner J, Wright B, Emberey J, Spencer P, Gillott R, Summers A, et al. Towards radiological diagnosis of abdominal adhesions based on motion signatures derived from sequences of cine-MRI images. Physica Medica. 2014 Jun 1;30(4):437–47.

25. Randall D, Joosten F, Ten Broek RP, Gillott R, Bardhan KD, Strik C, et al. A novel diagnostic aid for intra-abdominal adhesion detection in cine-MRI: pilot study and initial diagnostic impressions. BJR [Internet]. 2017 Jul 14 [cited 2020 Mar 26];90(1077). Available from: https://www.birpublications.org/doi/full/10.1259/bjr.20170158

26. Tustison NJ, Avants BB, Cook PA, Zheng Y, Egan A, Yushkevich PA, et al. N4ITK: Improved N3 Bias Correction. IEEE Transactions on Medical Imaging. 2010 Jun;29(6):1310–20.

27. Jourdan A, Troter AL, Daude P, Rapacchi S, Masson C, Bège T, et al. Semiautomatic quantification of abdominal wall muscles deformations based on dynamic MRI image registration. NMR in Biomedicine. 2021;34(4):e4470.

28. Ogier A, Sdika M, Fouré A, Le Troter A, Bendahan D. Individual muscle segmentation in MR images: A 3D propagation through 2D non-linear registration approaches. In: 2017 39th Annual International Conference of the IEEE Engineering in Medicine and Biology Society (EMBC). 2017. p. 317–20.

29. Walt S van der, Schönberger JL, Nunez-Iglesias J, Boulogne F, Warner JD, Yager N, et al. scikit-image: image processing in Python. PeerJ. 2014 Jun 19;2:e453.

30. Tustison NJ, Avants B avants. Explicit B-spline regularization in diffeomorphic image registration. Front Neuroinform [Internet]. 2013 [cited 2020 Jun 10];7. Available from: https://www.frontiersin.org/articles/10.3389/fninf.2013.00039/full

31. Urquhart DM, Barker PJ, Hodges PW, Story IH, Briggs CA. Regional morphology of the transversus abdominis and obliquus internus and externus abdominis muscles. Clinical Biomechanics. 2005 Mar 1;20(3):233–41.

32. Campbell EJM. An electromyographic study of the role of the abdominal muscles in breathing. J Physiol. 1952 Jun 27;117(2):222–33.

33. Tee M, Noble JA, Bluemke DA. Imaging techniques for cardiac strain and deformation: comparison of echocardiography, cardiac magnetic resonance and cardiac computed tomography. Expert Review of Cardiovascular Therapy. 2013 Feb 1;11(2):221–31.

34. Lee H-J, Lee K-W, Takeshi K, Lee Y-W, Kim H-J. Correlation analysis between lower limb muscle architectures and cycling power via ultrasonography. Sci Rep. 2021 Mar 8;11(1):5362.

35. Chen Y-Z, Yan S-Y, Chen Y-Q, Zhuang Y-G, Wei Z, Zhou S-Q, et al. Noninvasive monitoring of intra-abdominal pressure by measuring abdominal wall tension. World J Emerg Med. 2015;6(2):137–41.

36. Konerding MA, Bohn M, Wolloscheck T, Batke B, Holste J-L, Wohlert S, et al. Maximum forces acting on the abdominal wall: Experimental validation of a theoretical modeling in a human cadaver study. Medical Engineering & Physics. 2011 Jul 1;33(6):789–92.

37. Timmins RG, Shield AJ, Williams MD, Lorenzen C, Opar DA. Architectural adaptations of muscle to training and injury: a narrative review outlining the contributions by fascicle length, pennation angle and muscle thickness. Br J Sports Med. 2016 Dec;50(23):1467–72.

38. Weston AD, Korfiatis P, Kline TL, Philbrick KA, Kostandy P, Sakinis T, et al. Automated Abdominal Segmentation of CT Scans for Body Composition Analysis Using Deep Learning. Radiology. 2019 Mar 1;290(3):669–79.